European Journal of Medicinal Chemistry 50 (2012) 416–427

Contents lists available at SciVerse ScienceDirect

European Journal of Medicinal Chemistry

journal homepage: http://www.elsevier.com/locate/ejmech

Original article

Synthesis and characterization of pH-responsive and folated nanoparticles based on self-assembled brush-like PLGA/PEG/AEMA copolymer with targeted cancer therapy properties: A comprehensive kinetic study

Sepideh Khoee*, Reza Rahmatolahzadeh

Polymer Chemistry Department, School of Science, University of Tehran, PO Box 14155-6455, Tehran, Iran

ARTICLE INFO

Article history:
Received 16 August 2011
Received in revised form
2 February 2012
Accepted 14 February 2012
Available online 22 February 2012

Keywords:
Amphiphilic brush-like copolymer
pH sensitivity
Core-shell nanoparticles
Targeting
Degradation study

ABSTRACT

In this study, a novel nanocarrier was synthesized based on methacrylated poly(lactic-co-glycolic acid) (mPLGA) as a lipophilic domain, acrylated methoxy poly(ethylene glycol) (aMPEG) as hydrophilic part and *N*-2-[(tert-butoxycarbonyl)amino] ethyl methacrylamide (Boc-AEMA) as pH-responsive segment. Radical polymerization of the above-mentioned three modified monomers produces amphiphilic brush-like copolymer. The protecting amine group (Boc) was selectively deprotected and the latter targeted copolymer was produced through the reaction of this copolymer with activated folic acid. Nano-precipitation method was used to prepare quercetin-loaded nanoparticles. Dynamic light scattering (DLS) analysis showed that the produced nanoparticles had nanometric size (<100 nm) and low poly-dispersity in size at different pHs. Higuchi and Korsmeyer–Peppas models were applied to evaluate release mechanisms and kinetics. Based on in-vitro degradation study, we found that the brush-like copolymer underwent a rapid weight loss in acidic pH.

1. Introduction

Polymeric micelles have been developed as drug delivery systems as well as carriers for various contrasting agents in diagnostic imaging applications [1–5]. With the amphiphilic structure of the polymeric micelles, hydrophobic pharmaceutical compounds are solubilized within the hydrophobic cores, whereas the shell maintains a hydration barrier that protects the integrity of each micelle. As a result, polymeric micelles can be used as efficient containers for reagents with poor solubility and/or low stability in physiological environments [6–9]. Moreover, the ability to tailor its numerous end groups offers considerable scope for fine-tuning its drug loading and targeted drug release properties. Selective drug targeting to cancer cells is an interesting task [10–13]. This is especially true for chemotherapeutic cancer treatment because most anti-cancer drugs cannot distinguish between cancerous and healthy cells. A well-known approach to accomplish active tumor targeting is to chemically link specific ligands to the micelle's outer layer that can recognize the exact molecular signatures of the cancer cells. To increase drug delivery efficiency and specific cancer therapy, a strong attention has been paid to develop drug carriers with active targeting ability. Moreover, tissue specificity is another issue for design of an appropriate carrier. Among various targeting moieties, such as peptide and antibody [14–17], which can be recognized and bind to specific receptors that are unique to cancer cells, the folate receptor is vastly over-expressed in a wide variety of human tumor cells [18–21]. Drug targeting can also be achieved by using a polymer that is sensitive to the surrounding temperature or pH [22–25]. Various stimuli such as ultrasound, light, or micro-environmental changes in temperature and pH could affect on stimuli-responsive polymeric micelles. Due to their ability to release their encapsulated drugs at specific sites where the stimuli are present, they are known as 'smart' delivery systems. The pH-responsive polymeric micelles and nanoparticles are particularly useful for application in biological systems because of the numerous pH gradients that exist in both normal and pathophysiological states.

In this work, we describe the synthesis and micellar characterization of folated and non-folated amphiphilic brush copolymers based on methacrylated poly(lactic-co-glycolic acid) (mPLGA) as the hydrophobic segment which are biodegradable and extensively used in therapeutic devices. Acrylated methoxy poly(ethylene glycol) (aMPEG) chains, as hydrophilic domain placed on the micelle surface can protect the nanocarrier from undesired attacks

* Corresponding author. Tel.: +98 21 61113301; fax: +98 21 6649 5291.
E-mail address: Khoee@Khayam.ut.ac.ir (S. Khoee).

0223-5234/$ – see front matter © 2012 Elsevier Masson SAS. All rights reserved.
doi:10.1016/j.ejmech.2012.02.027

in the biological media. Thereby increasing the stability of micelles and prolonging their circulation time in the blood. 2-Aminoethyl methacrylamide (AEMA), with a primary amine group is expected to play dual role. A crucial role in offering the pH sensitivity to the produced nanocarriers and also providing a site to conjugate folic acid to copolymer and make it suitable for targeted anti-cancer drug delivery. Since controlling the molar ratio of PLGA:MPEG:AEMA can affect physical properties of the final nanoparticles, the effective ratio of amphiphilic and pH-responsive copolymer should be tailored via addition copolymerization of the above modified monomers and hence the drug loading and release level of the resulting polymeric micelles can be adjusted. The AEMA groups can become hydrophobic and adhere tightly on the inner hydrophobic block at neutral pH or change to hydrophilic chains and create corona layer with PEG chains at acidic pHs. Changing in AEMA nature affects the drug release profile and to accurately investigate the drug release mechanism, the release data were fitted into exponential models such as Higuchi and Korsmeyer–Peppas. The relationship between copolymer compositions and the rate of copolymer degradation with core-shell architecture were also evaluated.

2. Experimental

2.1. Materials

Methoxy poly(ethylene glycol) (MPEG) ($M_w = 2000$) and D,L-lactic acid and glycolic acid, ethylene diamine (EDA), di-tert-butyl carbonate were purchased from Fluka Co (Switzerland). Acryloyl chloride, methacryloyl chloride, methacrylic anhydride, *N*-hydroxy succinimide (NHS), dicyclohexylcarbodiimide (DCC) and triethylamine (TEA), trifluoroacetic acid (TFA), folic acid (FA), 2,2-azobisisobutyronitrile (AIBN) were supplied from Sigma–Aldrich Co (USA). 1,2-dichloromethane, methanol, dimethyl sulfoxide (DMSO), 1,4-dioxane, Ethyl ether and acetone were purchased from Merck Co (Germany). AIBN was purified by recrystallization from hexane and acetone, respectively. Other reagents were commercially available and were used as received.

2.2. Methods

^{1}H NMR spectra were recorded in $CDCl_3$ solution on a Bruker (Germany) DRX 500 (500 MHz) apparatus with the TSM proton signal for reference. IR measurements were performed using a Bruker EQUINOX 55 model FT-IR. Dynamic light scattering experiments were performed with commercially available equipment (Zeta-sizer Nano from Malvern) [United Kingdom] using a 4-mW He–Ne laser (633 nm wavelength) with a fixed detector angle of 173°. Size and morphology of the nanoparticles were investigated by scanning electron microscopy (SEM) with Vega-II from Tescan Co (Brno, Czech Republic). The number average molecular weight (M_n) and the weight average molecular weight (M_w) of hybrid copolymer were estimated by gel permeation chromatography (GPC) (Agilent 1100) with THF as the mobile phase at 25 °C. Poly(styrene) standard samples were used for calibration.

2.3. Synthesis of monomers

2.3.1. Synthesis of acrylated PEG

Acrylated methyl ether poly(ethylene glycol) (ACMPEG) was synthesized with 73% yield according to the previously reported procedure (Scheme 1 – Step 3) [26].

2.3.2. Synthesis of PLGA

Polycondensation reaction of glycolic acid and D,L-lactic acid was performed according to the modified procedures described in reference in the presence of Sb_2O_3 and under nitrogen atmosphere [27,28]. Briefly, a pre-determined amount of D,L-LA and GA (70/30 of molar ratio) was charged into a two-necked round-bottomed flask equipped with nitrogen inlet and a condenser to transfer the produced water to the second two-necked round-bottomed flask which was equipped with nitrogen outlet. The flask was heated in an oil bath to 120 °C for an hour and then 180 °C for 5 h to melt the monomers. Accordingly, 85% of water was removed approximately, to increase the conversion, the temperature was lowered to 150 °C and reaction media was stirred for another 2 h. The ring-opening polymerization under nitrogen atmosphere continued for 12 h with stirring under vacuum at room temperature. After the reaction was completed, the product was dissolved in dichloromethane and then re-precipitated from an excess cold diethyl ether three times. The precipitate was dried under vacuum for 72 h to produce 15.2 g of PLGA (95.6% yield).

2.3.3. Synthesis of methacrylated PLGA

In a 250 mL three-necked round-bottomed flask, PLGA (4 g, 8.0×10^{-4} mol) was dissolved in dehydrated dichloromethane (20 mL) and cooled to 4 °C for 30 min. Next, triethylamine (0.5 mL, 3.73×10^{-3} mol) was added dropwise to the cold PLGA solution while stirring and the final solution was stirred for another 15 min. An excess amount of methacrylic anhydride (1.5 mL, 10.06×10^{-3} mol) was added to the reaction vessel, and the solution was stirred at room temperature under mild vacuum for 48 h. The mixture was filtered off to remove any sedimentation and then precipitated in cold methanol to produce methacrylated PLGA (3.0 g, 74% yield). The precipitate was dried under vacuum for 72 h.

2.3.4. Synthesis of N-2-[(tert-butoxycarbonyl)-amino] ethyl methacrylamide (Boc-AEMA)

Boc-AEMA was synthesized with 55% yield according to the previously reported procedure [29].

2.4. Synthesis of copolymers

2.4.1. Preparation of brush-like copolymer from acrylated and methacrylated monomers

Brush-like copolymer was synthesized by free radical copolymerization of the three modified monomers. Pre-determined amount of acrylated PLGA, methacrylated-MPEG, methacrylated-AEMA-BOC and AIBN (feed molar ratio of monomers to initiator was 100:6) was dissolved in 15 mL of dehydrated dichloromethane and placed in a three-necked round-bottom flask equipped with a magnetic stirrer, condenser and nitrogen inlet and outlet. The mixture was completely degassed by nitrogen gas for 20 min and then stirred under nitrogen blanket for 24 h at 65 °C. After polymerization, the product was purified by precipitation from petroleum ether twice to obtain 2.6 g (70.2% yield) of the copolymer.

2.4.2. Deprotection of t-BOC group from brush copolymer

BOC protecting group was removed by TFA. TFA (0.3 mL) was added to a solution of copolymer (1.0 g, 0.08×10^{-3} mol) in chloroform and ethyl acetate (14 mL, 1:6 mixture). The reaction was carried out for 1 h at room temperature under magnetic stirring. The reaction mixture was neutralized with 10% aqueous sodium bicarbonate solution (2×10 mL) and then washed with aqueous sodium chloride solution (2×10 mL). The organic layer was dried over $MgSO_4$, filtered and solvent was evaporated under reduced pressure to yield 0.54 g (55%) of the deprotected copolymer.

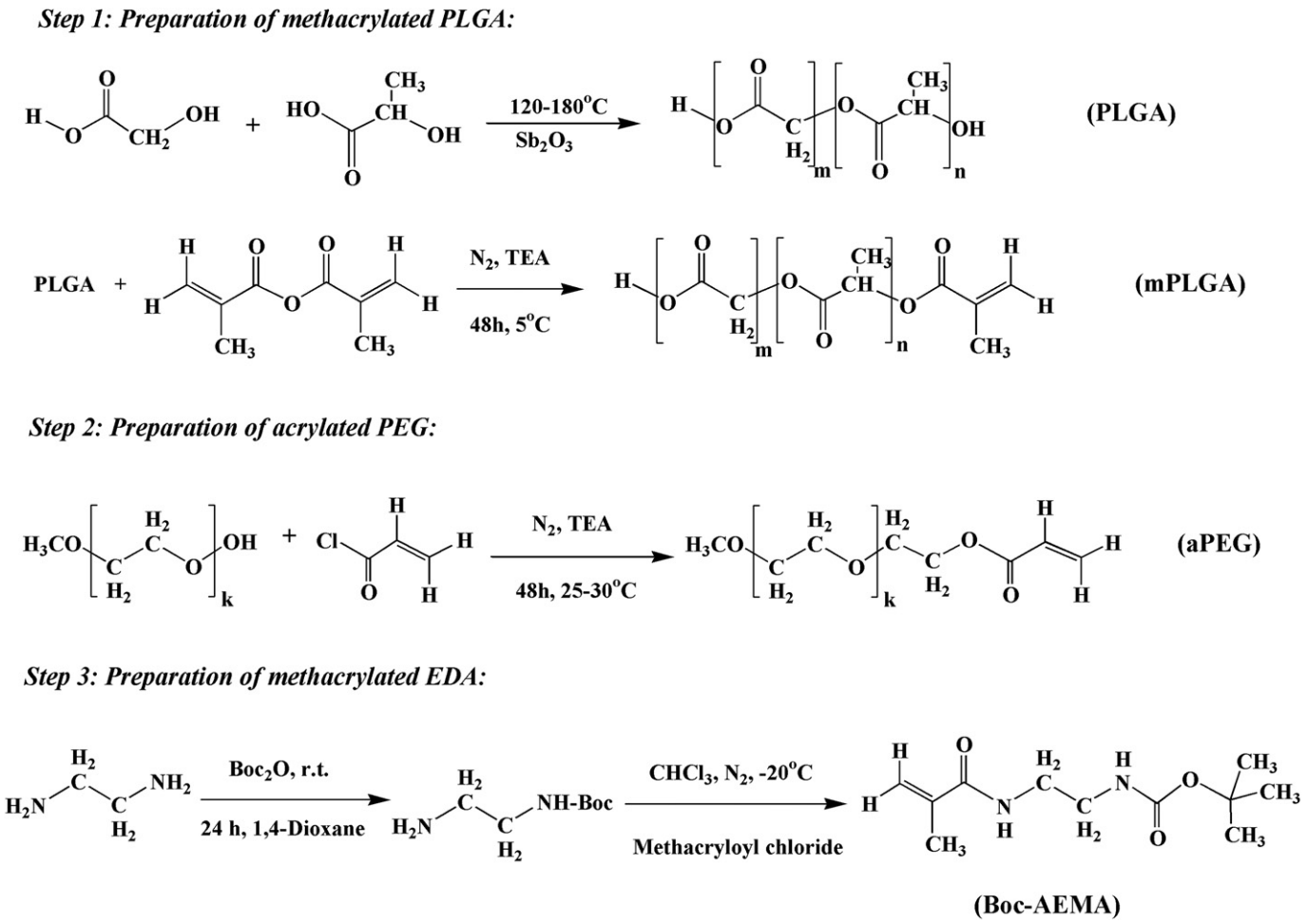

Scheme 1. Synthesis of methacrylated PLGA (mPLGA), acrylated PEG (aPEG) and methacrylated ethylene diamine (Boc-AEMA).

2.4.3. Synthesis of folate-copolymer

Folate conjugated copolymer was prepared within a two-step procedure: (1) carboxylation of folic acid with NHS to yield folate-NHS; (2) conjugation of copolymer with folate-NHS to produce folate-copolymer. The carbodiimide-activated folic acid can couple with either α- or γ-carboxyl group residue [30]. Reaction conditions were set to favor linkage with γ-carboxyl residue. A solution of folic acid (1 g, 2.2×10^{-3} mol) in anhydrous DMSO (25 mL) was reacted an overnight with NHS (0.9 g, 7.81×10^{-3} mol) in the presence of DCC (0.5 g, 2.4×10^{-3} mol) under argon at room temperature, and the major by product, 1,3-dicyclohexyllurea (DCU), was removed by filtration. Subsequently, the above activated folate solution (3 mL) was added to a solution of brush copolymer (0.4 g, 0.03×10^{-3} mol) in DMSO (5 mL) containing triethylamine (0.05 mL, 0.35×10^{-3} mol). The reaction was performed at room temperature for 10 h under argon atmosphere. The final product was centrifuged, filtered and purified by dialysis against deionized water for 24 h (molecular weight cut-off 2000 Da) and freeze-dried to produce 0.25 g (61% yield) folate conjugated polymer.

2.5. Preparation of drug-loaded micelles

Drug-loaded nanoparticles were prepared by nanoprecipitation. The brush copolymer (10 mg) and pre-determined amount of quercetin were dissolved in acetone (2 mL), and then the obtained organic solution was added dropwise to distilled water (10 mL) under stirring at room temperature and then, acetone was thoroughly removed under reduced pressure. Finally, the resulting aqueous dispersion was filtered through 0.2 μm cellulose acetate syringe filter to remove aggregated copolymers and non-incorporated drug crystals and then, freeze-dried to extract fine nanoparticles from the aqueous medium. Nanoparticles formed from folated copolymer carrier were prepared as below: folate conjugated brush copolymer (10 mg) and pre-determined amount of quercetin were dissolved in DMSO and acetone (3 mL, 1–8), then the obtained organic solution was added dropwise to distilled water (10 mL) at room temperature stirringly. Then, acetone was completely removed under reduced pressure. Finally, the resulting aqueous dispersion was filtered through 0.2 μm cellulose acetate syringe filter according to the above procedure.

2.6. Nanoparticle yield, drug loading and encapsulation efficiency

The nanoparticle yield was obtained by gravimetric method. Drug content in the nanoparticles was measured using a dissolution method. A pre-determined amount of the freeze-dried nanoparticles was dissolved in 5 mL of acetone. The concentration of quercetin was analyzed with ultraviolet absorption at their maximum wavelength (362 nm) on a UV spectrophotometer. Three

samples were prepared for each test. The nanoparticle yield, encapsulation efficiency (EE) and drug loadings (DL) were calculated using the following equations (Eqs. (1)–(3)):

$$\text{Nanoparticle yield}(\%) = \frac{\text{Weight of the nanoparticles}}{\text{Total weight of drug and copolymer}} \times 100 \quad (1)$$

$$\text{Drug loading}(\%) = \frac{\text{Weight of encapsulated drug}}{\text{Weight of the nanoparticles}} \times 100 \quad (2)$$

$$\text{Encapsulation efficiency}(\%) = \frac{\text{Weight of encapsulated drug}}{\text{Total weight of drug}} \times 100 \quad (3)$$

2.7. In-vitro drug release studies

The in-vitro release studies of quercetin-loaded nanoparticles were performed by diffusion technique. The nanoparticle suspension (10 mL) was placed into a pre-swelled dialysis bag that was immersed into phosphate buffer saline (PBS) solution (100 mL, pH = 7.4 and 5.8) at 37 °C. At pre-determined time intervals, the solution (3 mL) was taken out from the release media and replaced with fresh PBS (3 mL). Then the released drug was measured using UV spectra at 202 nm.

2.8. Mechanism of drug release

The release data were analyzed by model-dependent (curve fitting) methods. For model-dependent analysis, two theoretical models describing drug release from polymeric systems were used according to Higuchi [31] and Korsmeyer–Peppas [32]. Higuchi model describes drug release as a diffusion process based on Fick's law according to the following Eq. (4):

$$\frac{M_t}{M_\infty} = k\sqrt{t} \quad (4)$$

where k is a constant reflecting formulation characteristics, and M_t and M_∞ are cumulative amounts of released drug at time t and infinite time, respectively. According to this model, a straight line is expected for the plot of M_t/M_∞ versus the square root of time if the drug release from the matrix is based on a diffusion mechanism. The Korsmeyer–Peppas model is considered if the drug release mechanism deviates from Fick's law and follows an anomalous behavior described by the following equation:

$$\frac{M_t}{M_\infty} = k' t^n \quad (5)$$

where k' is the kinetic constant and n is an exponent, characterizing the diffusion mechanism. When pure diffusion obeys the controlling release mechanism, n equivalents to 0.5 and Eq. (5) coincide to Eq. (4). Moreover, Eq. (4) becomes physically realistic for $n = 1$ since the drug release follows swelling controlled release or Case II transport [33]. Both Eqs. (4) and (5) are short time approximations of complex exact relationships and therefore, their use is confined for the description of the first 60% of release curve. The n value is used to characterize different release mechanisms as given in Table 1 for the spherical shaped matrices.

Table 1
Diffusion exponent and solute release mechanism for spherical shape matrices.

Diffusion exponent (n)	Overall solute diffusion mechanism
$n < 0.43$	Fickian diffusion
$0.43 < n < 0.85$	Anomalous (non-Fickian) diffusion
$0.85 < n < 1$	Case II transport
$n > 1$	Super Case II transport

2.9. Statistical analysis

Particle diameters and "in-vitro" release analyses were performed in triplicate. The data are represented as mean ± standard deviation (SD). Data were analyzed using the T test and one-way analysis of variance (ANOVA) and considered significantly different at the level of $p < 0.05$.

2.10. Polymer degradation

For degradation study, polymeric nanoparticles were prepared using nanoprecipitation method. 10 mg ($n = 3$) of the synthesized polymer was dissolved in 2 mL of acetone and then the dissolved polymer was added dropwise to 10 mL of phosphate buffer (pH 7.4 and 5.8) under stirring at room temperature and then, acetone was thoroughly removed under reduced pressure. Weight loss of water insoluble amine-modified brush copolymer was measured gravimetrically after incubation of polymer nanoparticles in phosphate buffered saline over 5 weeks. After 4, 12 and 36 days, samples were freeze-dried and then were carefully washed five times with distilled water to remove the salt residues. The recovered samples were dried in a vacuum oven for approximately 3 days at room temperature until constant masses were obtained. Polymer total residue was calculated from the following formula:

$$\text{Total residue}\ (\%) = \frac{\text{Final weight of a dried sample}}{\text{Original weight}} \times 100$$

The morphology of polymer nanoparticles was characterized by SEM.

3. Result and discussion

3.1. Design, synthesis and characterization of the brush copolymer

The polymer structure containing two types of polymer chains was a brush-like copolymer prepared by macromer copolymerization. The acrylated macromer of PEG and methacrylated macromer of PLGA, and monomer of EDA was prepared separately according to Scheme 1. The core of the micelles consisted of hydrophobic chain of PLGA copolymer to make it biodegradable. Synthesis of the poly(lactic-co-glycolic acid) macromer has been presented in Scheme 1, step 1. Sb_2O_3, as a Lewis acid, acts as the catalyst for the esterification reaction. Number (M_n) and weight (M_w) average molecular weights of PLGA were determined by GPC and were 2280 and 5396 g/mol respectively with PDI of 2.36.

The secondary hydroxyl group of PLGA reacted efficiently with methacrylic anhydride in the presence of triethylamine to provide the methacrylated PLGA (mPLGA) macromer. The structure of this macromer that contains a double bond group was characterized with ^{1}H NMR (Fig. 1a) and FT-IR (their data was not shown) spectroscopy.

The peak "a" was attributed to the methylene protons of the glycolic acid segment and peaks "b" and "c" were assigned to the methyne and pendent methyl protons of lactic acid domain, respectively.

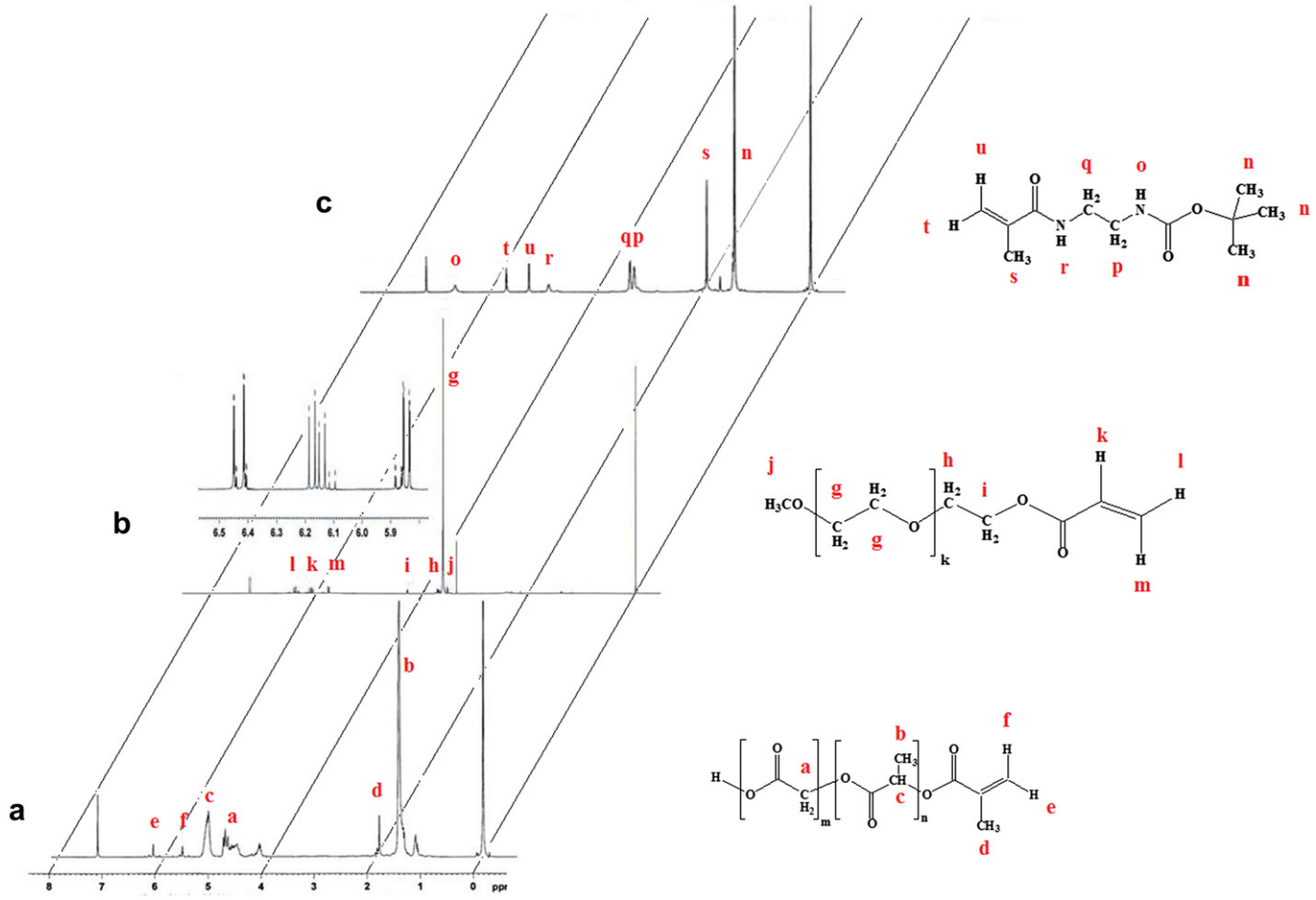

Fig. 1. ^{1}H NMR spectra of (a) methacrylated PLGA (mPLGA) macromer, (b) acrylated PEG (aPEG) macromer and (c) methacrylated ethylene diamine (Boc-AEMA) monomer.

In order to make the copolymer more compatible with biological systems, we have designed hydrophilic polyethylene glycol-2000 was modified to be incorporated into the copolymer chain (Scheme 1, step 2). Fig. 1b displays the spectrum of acrylated PEG and peaks "g", "h", "i", and "j" were attributed to the methylenic PEG groups. The expanded region for "l", "k" and "m" peaks of the acrylic group has been demonstrated, which reveals the preparation of modified PEG macromer.

N-2-[(tert-butoxycarbonyl)-amino] ethyl methacrylamide (Boc-AEMA) is a pH-sensitive monomer which can be synthesized successfully by consecutive protection and deprotection of one of the two amino groups of ethylene diamine. Boc-AEMA has the necessary features as a carrier for the development of targeted anticancer delivery systems. It also possesses the versatility of facile modification and functionalization of folate nanoparticles via the amino groups to achieve dual-targeted nanocarriers. Boc-AEMA was synthesized from the reaction of methacryloyl chloride with *N*-2-[(tert-butoxycarbonyl)-amino] ethyl amine according to the previously reported procedure (Scheme 1, step 3) [29]. Fig. 1c shows the ^{1}H NMR spectra of methacrylated-EDA (Boc-AEMA) monomer. Peaks "o", "p", "q", "r", "s", "t", "u" and "n" were assigned to the AEMA and terminal methyl protons of the Boc-AEMA pendant group, respectively.

The modified monomers were copolymerized using free radical copolymerization according to Scheme 2. The brush-like amphiphilic copolymers with different compositions were synthesized by varying ratios of the three components in the initial mixture as well as AIBN amount (Table 2). Due to ambivalent nature of copolymers, the new hydrophilic/hydrophobic material has an improved properties compared with the initial modified monomers. Consequently, the smallest nano-sized formulation has been selected for drug carrier.

The structure of resulting brush-like copolymer that contained three modified monomers was determined by ^{1}H NMR spectroscopy. The composition of each grafted group in the soluble copolymer was measured by the integral of characteristic peaks of PLGA (at 5.18 ppm), PEG (at 3.65 ppm) and Boc-AEMA (at 3.39 ppm) (Fig. 2a). According to this calculation, the average number of each monomer in the targeted brush-like copolymer was about 1 PLGA macromer, 2 PEG macromers and 11 Boc-AEMA monomers in the repeating unit. Therefore the molecular weight of corresponding copolymer should be around 12 kDa, which is responsible for the formation of smaller-size nanomicelles.

Table 2
Chemical composition and physicochemical properties of brush-like copolymers.

PLGA/PEG/AEMA[a]	AIBNHY[b](%)	Encapsulation efficiency (%)	Particle size (nm)
2/2/12	3	70.1	337
2/2/12	6	62.4	190
1/2/12	3	57.3	159
1/2/12	6	54.0	84

[a] Feed molar ratio of monomers.
[b] The molar ratio of initiator to total monomers.

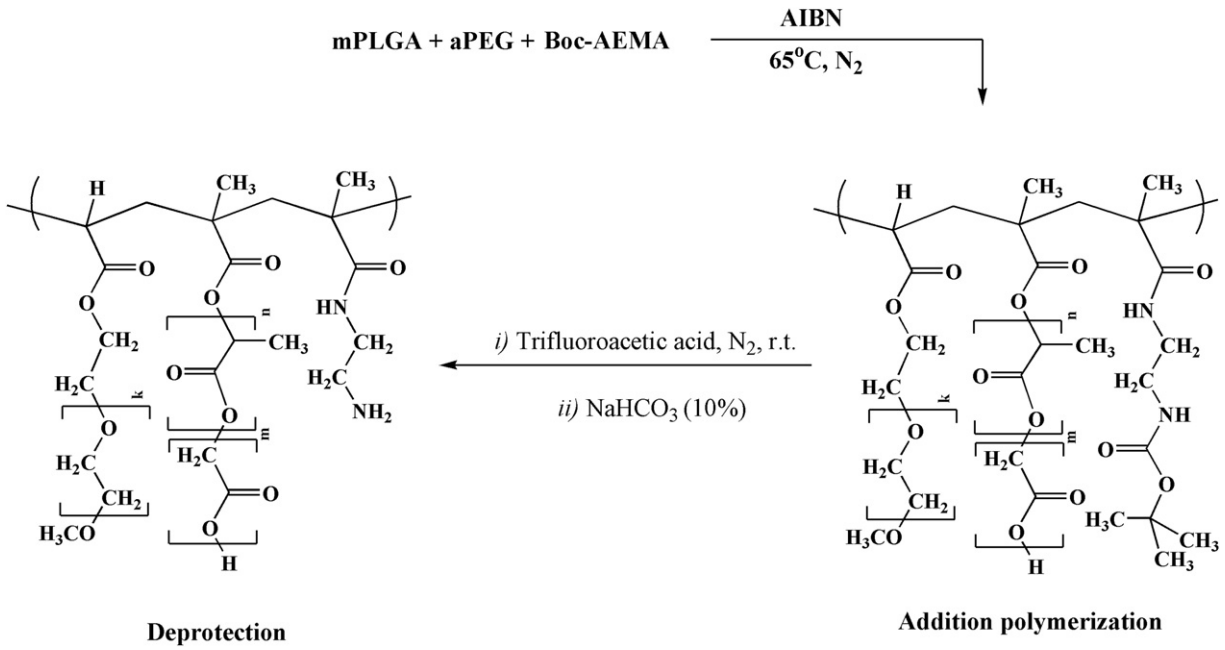

Scheme 2. Preparation of amphiphilic brush copolymer via addition copolymerization.

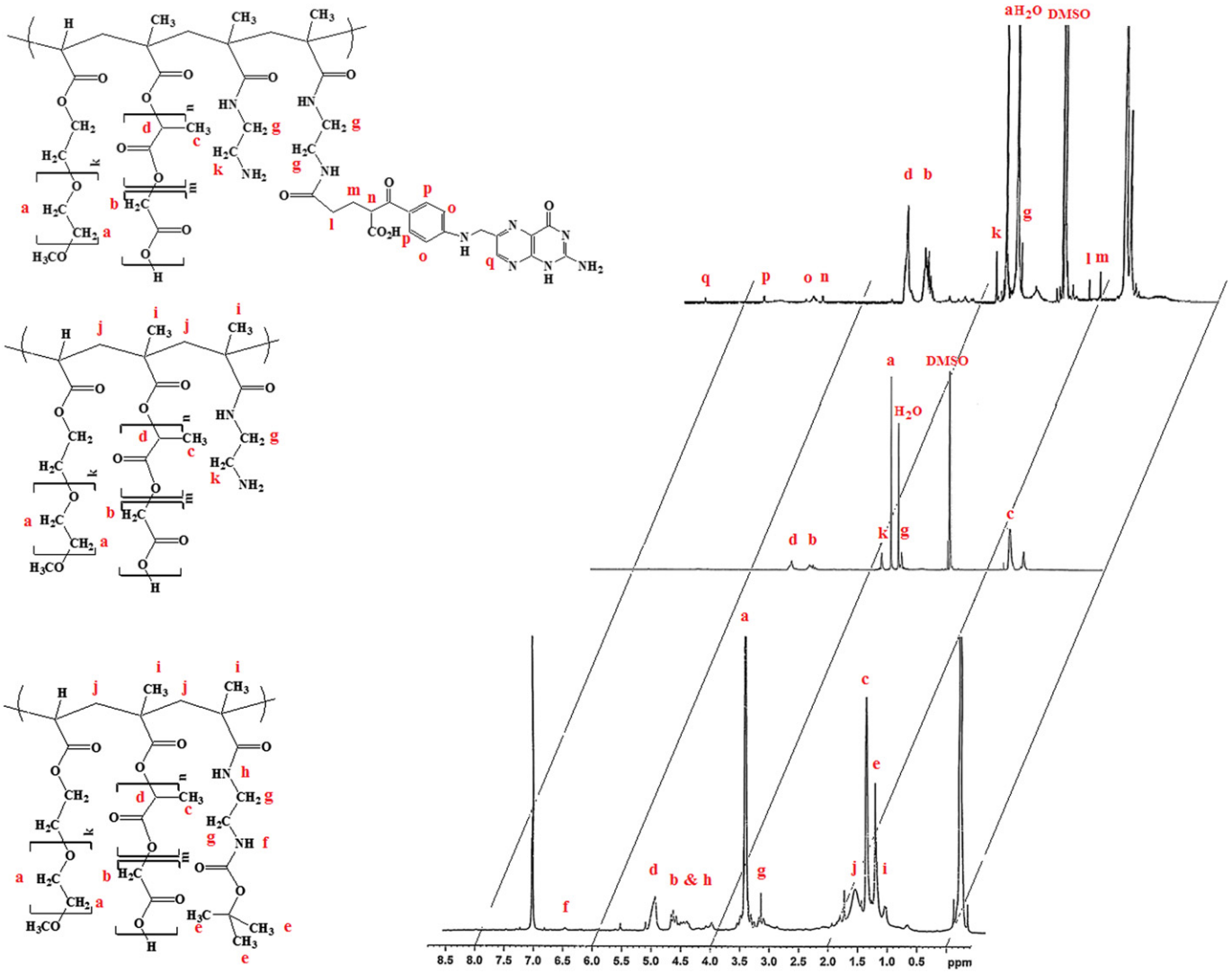

Fig. 2. ^{1}H NMR spectra of (a) t-Boc-protected brush copolymer, (b) deprotected brush copolymer and (c) folate targeted brush copolymer.

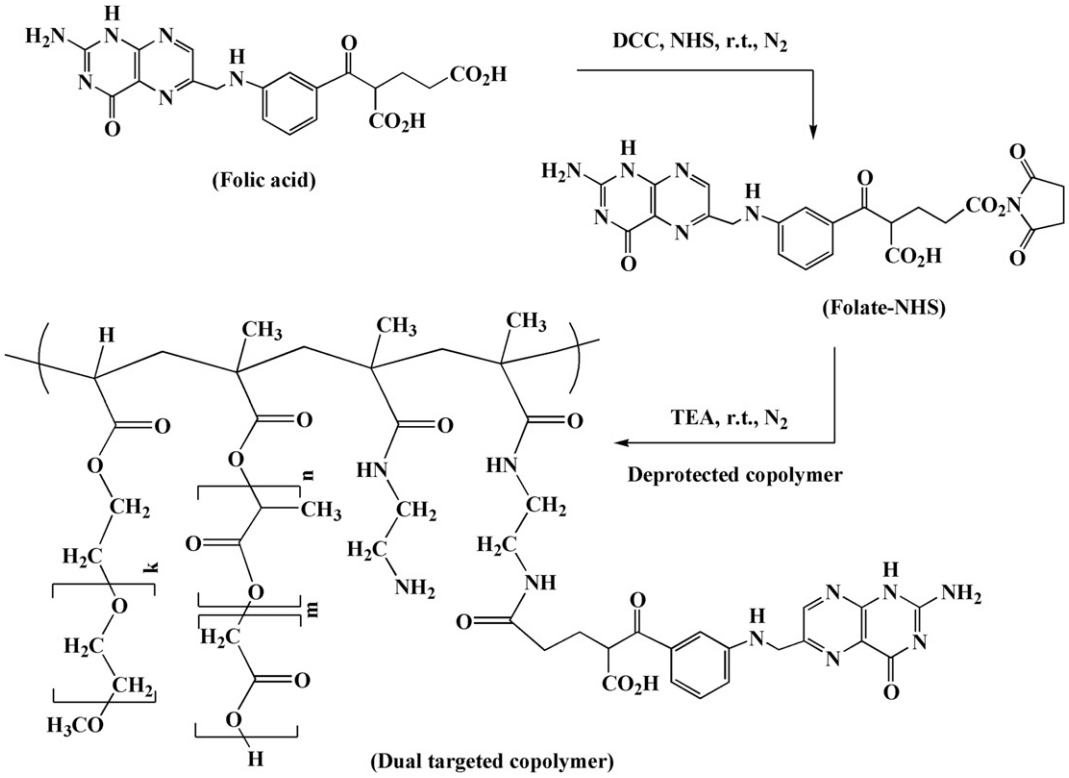

Scheme 3. Synthetic route for preparation of dual-targeted brush-like copolymer.

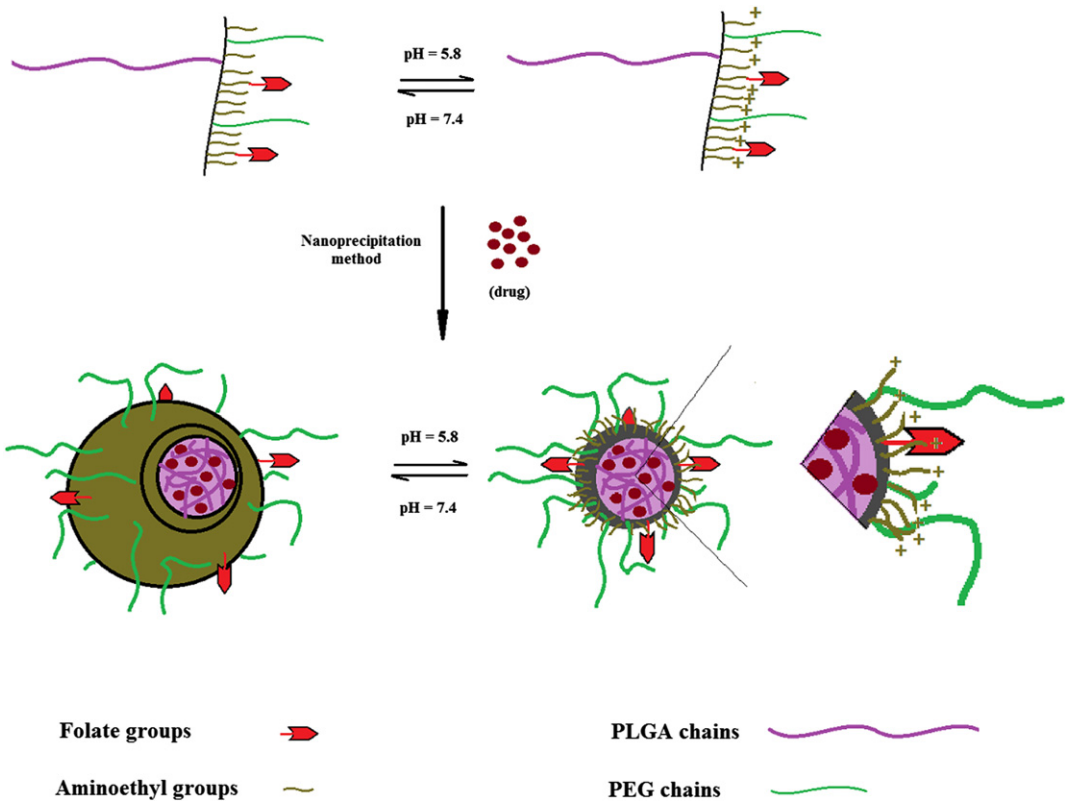

Scheme 4. Schematic representation of preparation of the drug-loaded pH-responsive nanoparticles.

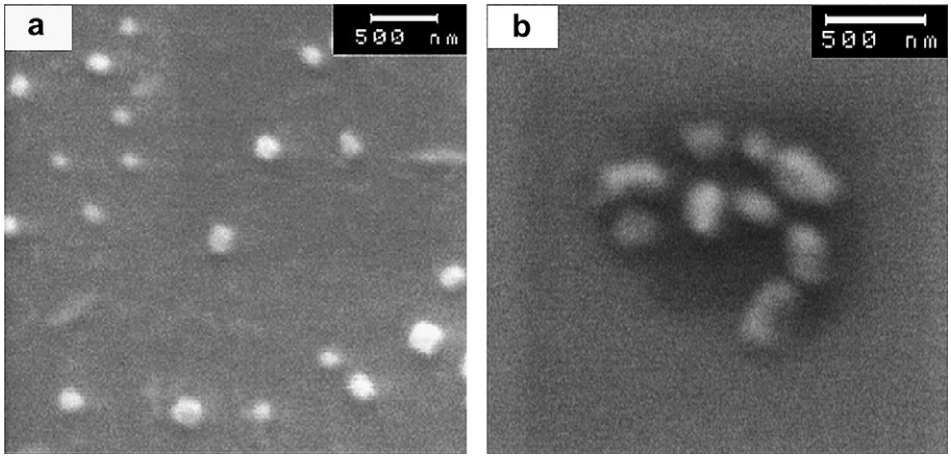

Fig. 3. SEM images of non-folated nanoparticles at pH 5.8 (a) and pH 7.4 (b).

Here, mono-Boc-protected copolymer was converted into the corresponding amino-terminated copolymer. Deprotection of t-Boc group was carried out in trifluoroacetic acid/chloroform and ethyl acetate solvent mixture (v/v, 0.3/14) for 1 h at room temperature. Disappearance of the *tert*-butyl peak at 1.45 ppm of ^{1}H NMR spectrum (Fig. 2b) depicts complete removal of the Boc group.

As shown in Scheme 3, deprotected brush-like copolymer was then coupled with activated folic acid by using of DCC. Folate-NHS was prepared to activate the folate carboxylic groups for coupling with terminal amino groups of the AEMA. The reaction between folate-NHS with the terminal amine in deprotected copolymer led to the formation of a covalent amide bond. The degree of substitution was evaluated to be 91% from ^{1}H NMR by considering the integral of the NH_2 protons of deprotected AEMA ($\delta = 3.67$) to the PEG backbone protons ($\delta = 3.51$) (Fig. 2c).

3.2. Nanoparticle preparation

The nanoparticles were prepared in a single step by nano-precipitation method. The fabrication of the nanoparticle is shown in Scheme 4. The brush-like copolymer was firstly dissolved in acetone and DMSO as organic solvent and then dispersed in water to produce corresponding micellar nanoparticles.

3.3. Size and morphology of the brush-like copolymer micelles

Fig. 3 shows the SEM photographs of non-folated nanoparticles at different pHs. Shape of the micelles at pH 5.8 was almost spherical and the sizes were below 100 nm in diameter (Fig. 3a), whereas at pH 7.4, a morphological change from spherical to bean-like shape with a huge increase in size was observed. At pH 7.4, the nanoparticles were neutral but gradually became positively charged with decreasing pH to 5.8. This suggests that at low pHs, the AEMA chains become positively charged and correspondingly, the nanoparticles are arranged individually due to the electrostatic repulsion. As the surrounding pH increased, AEMA was deprotonated and their tendency to get together was increased; this led to the association of nanoparticles and conversion of their morphology to bean-like (Fig. 3b).

Fig. 4 shows particle size distribution of folated and non-folated micelles by DLS. The DLS results revealed that the mean size of folated nanoparticles was larger than non-folated ones. By adding folate to the copolymer structure, the diameter of nanoparticles increased from 75 nm to 84 nm with increasing their dispersity from 0.081 to 0.193 (Table 3).

Decreasing of pH could make nanoparticles bigger again, so the nanoparticles have a pH-dependent size as shown in Fig. 4. The difference in size between DLS and SEM results is due to the fact that DLS gives the hydrodynamic radius, which strongly depends on the surface charge. In acidic media, surface charge density increases and consequently, its mean hydrodynamic size increases. The zeta potentials of the nanoparticles in different pH have been measured to determine the stability and the surface charge of the nanoparticles. The absolute values of zeta potential for nanoparticles at pH 7.4 and 5.8 are −17.54 and −9.54 mV respectively. This means that the absolute zeta potential value decreases with decreasing pH of the medium and colloidal nanoparticles tend to aggregate and result in larger particles. As confirmed by Scheme 4 at pH 5.8, the AEMA chains were protonated and became water soluble. The hydrophobic PLGA chains with hydrophobic drug molecules associated as the hydrophobic core with the PEG and protonated AEMA as the corona. After the solution pH rose to 7.4, the AEMA chains were deprotonated, became hydrophobic and thus collapsing on the PLGA core as the hydrophobic middle layer. The PEG chains formed the hydrophilic corona too.

3.4. Drug loading into the folated and non-folated nanoparticles

Quercetin is a potent anti-cancer drug with poor water solubility. Quercetin was loaded into the nanoparticles by a nano-precipitation method. EE of the folated nanoparticles was found to be higher than that of non-folated ones, which may be due to the

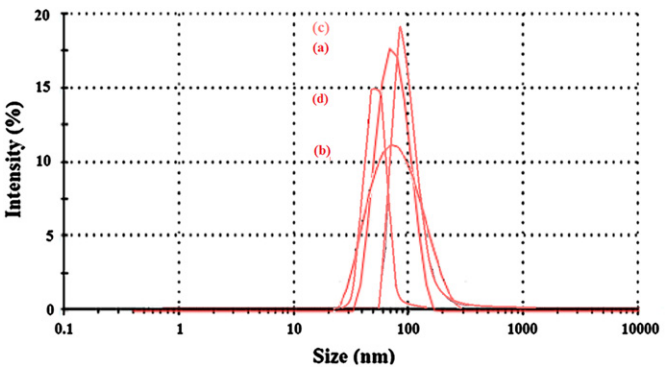

Fig. 4. Size of non-folated (a), folated (b) micelles at pH 7.4 and folated (c) micelles at pH 5.8.

Table 3
Particle size, drug loading, and encapsulation efficiency of copolymeric micelles in aqueous solution.

Nanoparticles	Drug/copolymer ratio in feed (%)	Yield (%)	Drug loading (%)	Particle size (nm)	Encapsulation efficiency (%)
Non-folated	15	53	12.58	75	54
Folated	15	62	13.7	84	58

drug–folate interactions. The drug loading into the folated copolymer was as high as 13.7% with an encapsulation efficiency of 58%, while the EE amount of non-folated copolymer could reach up to 54% with 12.58% drug loading. This comparison confirms that the folated nanoparticles are more effective for encapsulating the hydrophobic drug, which may be due to the establishment of the strong interactions between folate and drug functional groups.

The correlation between drug–folate interactions and EE amount has been recognized by UV–Visible spectrophotometer. As shown in Fig. 5, free quercetin displays two major absorption bands in the UV/Vis region. The broad peak with a maximum at 380 nm belongs to 10πe due to the contribution of π electrons from –OH group till carbonyl group (blue line) and a narrower peak with a maximum at 258 nm corresponds to hydroxyl substitutions on the benzene rings. Non-folated copolymer doesn't show any specific absorption in its UV/Vis spectrum due to the absence of conjugated chromophore and allowed transitions in copolymer structure. Folated copolymer shows their maximum absorption at 281 nm related to the $n \rightarrow \pi^*$ transitions by 6πe resonance system as shown in Fig. 5 and Scheme 5. The UV spectrum of quercetin-loaded folated nanoparticles exhibits an approximately 12 nm hypsochromic shift. This blue shift with an intense increase in the absorbance is caused by the decrease in conjugated system length and $\pi \rightarrow \pi^*$ transitions, respectively. It is observed that charge transfer complex (CT complex) formation between folate group of the copolymer and quercetin could convert the forbidden $n \rightarrow \pi^*$ transitions to the allowed $\pi \rightarrow \pi^*$ ones. This conversion leads to producing an α,β-unsaturated ketone with different chromophores at β position. In contrary, disappearance of the quercetin broad peak at 380 nm (10πe) after CT complex formation is due to the hiding of this peak in the folate one according to the low quercetin concentration in nanoparticles formulation.

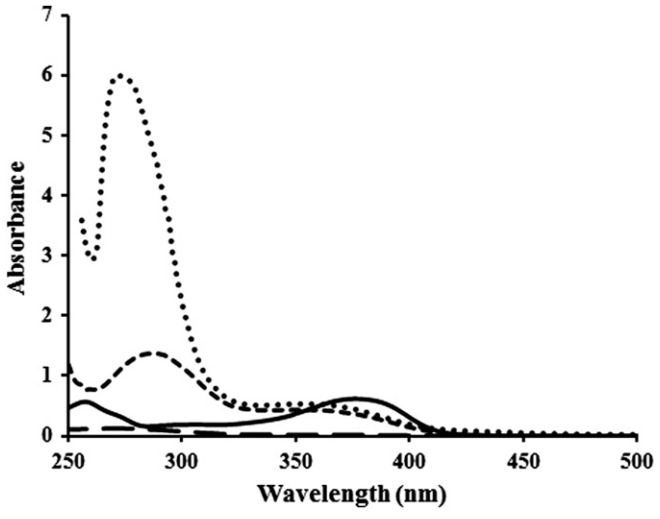

Fig. 5. UV–Vis spectra of free quercetin (——), non-folated copolymer (— —), folated copolymer (– – –) and quercetin-loaded folated nanoparticles (·····) in DMSO.

3.5. Release of quercetin from folated and non-folated nanoparticles

In-vitro drug release studies were carried out in various pH in order to evaluate the effect of pH on quercetin-release profile. The cumulative release of drug from the quercetin-loaded folated and non-folated copolymer in pH 5.8 and 7.4 at 37 °C has been shown in Fig. 6. Quercetin release from both copolymers was pH-dependent. The drug release rate at pH 5.8 was much faster than that of pH 7.4. The results indicate a conformational change in AEMA chains from a compacted shape to an expanded one with a decrease in the pH values. In expanded conformation, drug can diffuse out from the nanoparticles easier than in compacted form and the release rate of entrapped drug in the compacted form is reduced by condensed polymeric layers. Furthermore, drug release from non-folated nanoparticles in comparison with the folated one at both pH was slightly slower. The faster drug release of quercetin from the folated nanoparticles is due to the hydrophilicity of folic acid and its folate form. This property facilitates the water uptake of nanoparticles and causes a faster drug release. Hence, it is important to note that, this kind of copolymer has potential targeting capability as well as negligible effect on the rate of drug release.

3.6. Release kinetics and mechanism of quercetin-loaded nanoparticles

To investigate the kinetics of drug release from folated and non-folated nanoparticles, the plots of accumulated drug release as a function of the square root of time at pH 5.8 and 7.4 were plotted (Fig. 7).

Linear relationship is an indicative of diffusion-controlled mechanism for drug release from the polymeric nanocarrier. Release profiles from quercetin-loaded nanoparticles at pH 7.4 had minimum 2 h delay in comparison with similar nanoparticles at pH 5.8 and this was due to the protection of the AEMA-middle layer at higher pH. All release profiles show two release-stages i) first release-stage that is characterized by the steeper linear region, and ii) second release-stage that is characterized by the second linear region occurring at later time. The slopes of these linear regions for the polymer samples show that the kinetic of release for the first stage at different pH are obviously different, but that of the second stage are completely similar. This means that only the first step of release is affected by surrounding pH and the second one remains unaffected. To prove this claim, the release data were analyzed on the basis of Higuchi equation and Korsmeyer–Peppas kinetics. The release rates, $\boldsymbol{k}$ and $\boldsymbol{n}$ of each model were calculated by linear regression analysis using Microsoft Excel 2007 software. Coefficients of correlation (r^2) were used to evaluate the accuracy of the fit. The r^2, $\boldsymbol{n}$ and $\boldsymbol{k}$ values have been given in Table 4.

Based on the calculations and comparing r^2 values for Higuchi model, all formulations except the fourth one, gave good fit to the Higuchi model. According to this model, the drug release from these nanoparticles may be controlled by nanopore diffusion. All carriers were best fitted into the Korsmeyer–Peppas model and both nanoparticles showed a Fickian release at second stage of pH 5.8 and pH 7.4. Fickian drug release is identified by a linear

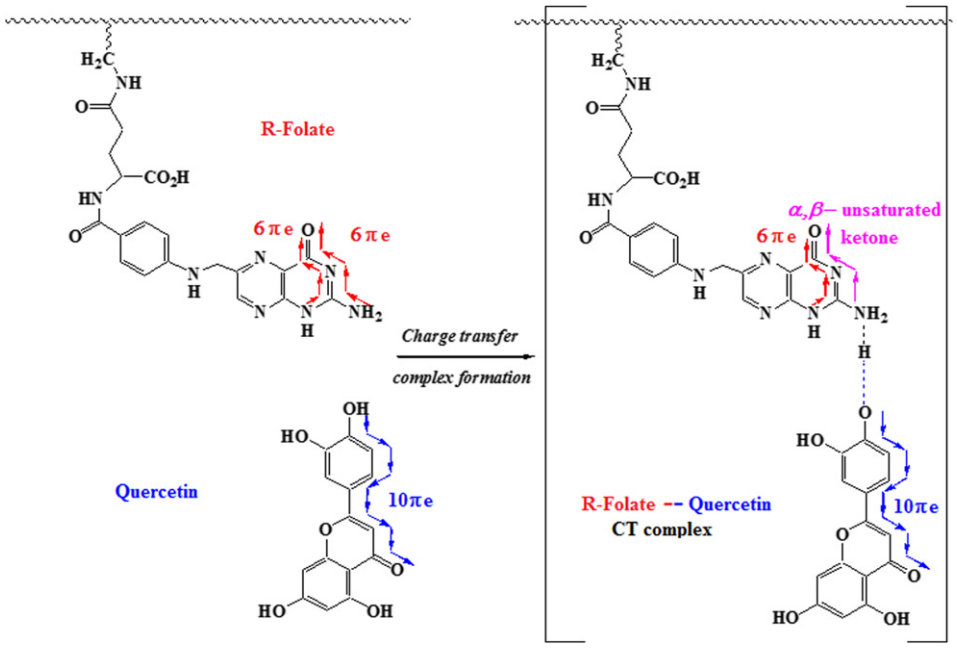

Scheme 5. The structure of quercetin, folated copolymer (left) and folated copolymer–quercetin charge transfer complex (right).

dependency of the released drug with the square root of time that is concentration dependent. The fundamental of diffusion is based on Fick's laws, which describes the macroscopic transport of molecules by a concentration gradient. These nanoparticles showed a non-Fickian or anomalous release in the first stage of both pHs and the drug release varies with time ***t*** according to the power law.

As, degradation rate depends on the pH of the in-vitro medium, additional experiments were carried out to investigate the degradation of amine-modified brush-like copolymer in buffer solution (PBS) at the desired pH values (5.8 and 7.4). In general, two mechanisms are considered for degradation of polymers: i) bulk erosion and ii) surface erosion. It is well-known that bulk erosion is the degradation process of PLGA and acidic conditions catalyze this kind of degradation [34]. In surface erosion, degradation mechanism proceeds from the outside to the inside with no reaction occurring in the core [35]. Fig. 8 shows the weight change and SEM pictures of in-vitro degradation of folated brush-like copolymer in pH 7.4 and 5.8. It can be seen that this copolymer has a slow degradation over 5 weeks period and at both pHs. The reason for observing this phenomenon may be the decrease in molecular weight of hydrophobic parts and subsequently, the short polymer chains may have less chance to be attacked by water molecules which is required for polymer chain hydrolysis or biodegradation [36]. For these nanoparticles, the patterns of mass loss were divided into two phases. During the initial 4 days, the rate of mass loss is almost similar for both pH media and after that, the rate of mass loss at pH 5.8 in comparison with pH 7.4 is increased. During 5

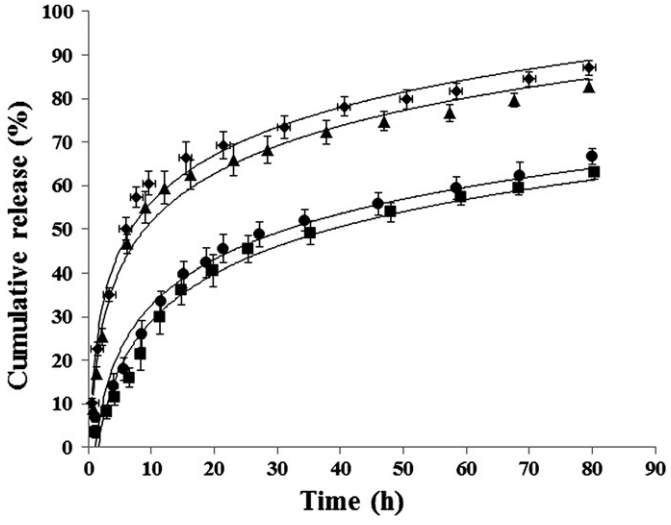

Fig. 6. In-vitro release profiles of quercetin from folated nanoparticles (at pH 5.8 (◆) and 7.4 (●)) and non-folated nanoparticles (at pH 5.8 (▲) and 7.4 (■)) at 37 °C ($n = 3$).

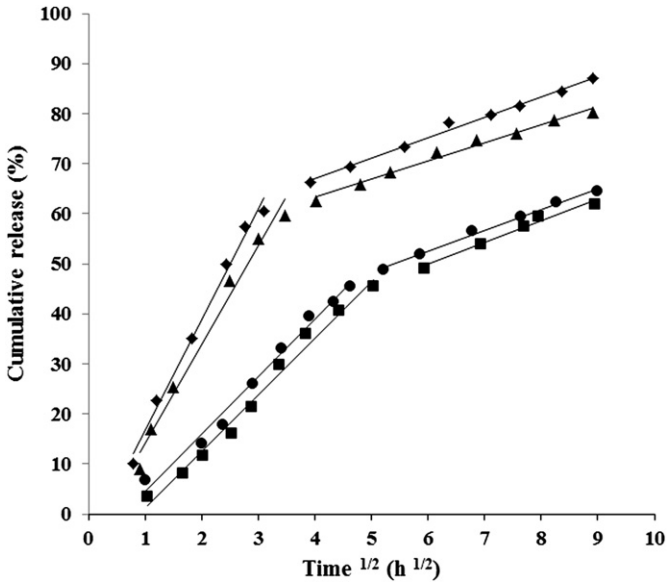

Fig. 7. The accumulated quercetin release from folated nanoparticles (at pH 5.8 (◆) and 7.4 (●)) and non-folated nanoparticles (at pH 5.8 (▲) and 7.4 (■)) at 37 °C as a function of the square root of time ($n = 3$).

Table 4
Statistical values for the release rate modeling.

Entry	Nanoparticles	pH	Stage	Higuchi		Korsmeyer–Peppas			Release mechanism
				k	r^2	***k'***	r^2	n	
1	Non-folated	5.8	1st	19.765	0.984	1.1997	0.991	0.559	Anomalous
2			2nd	3.642	0.984	1.6024	0.997	0.1597	Fickian
3		7.4	1st	11.379	0.986	0.5523	0.992	0.8262	Anomalous
4			2nd	4.33	0.977	1.2577	0.997	0.2814	Fickian
5	Folated	5.8	1st	22.128	0.991	1.2621	0.999	0.560	Anomalous
6			2nd	4.098	0.993	1.6194	0.997	0.1671	Fickian
7		7.4	1st	11.447	0.987	0.7029	0.990	0.7492	Anomalous
8			2nd	4.158	0.994	1.3105	0.998	0.263	Fickian

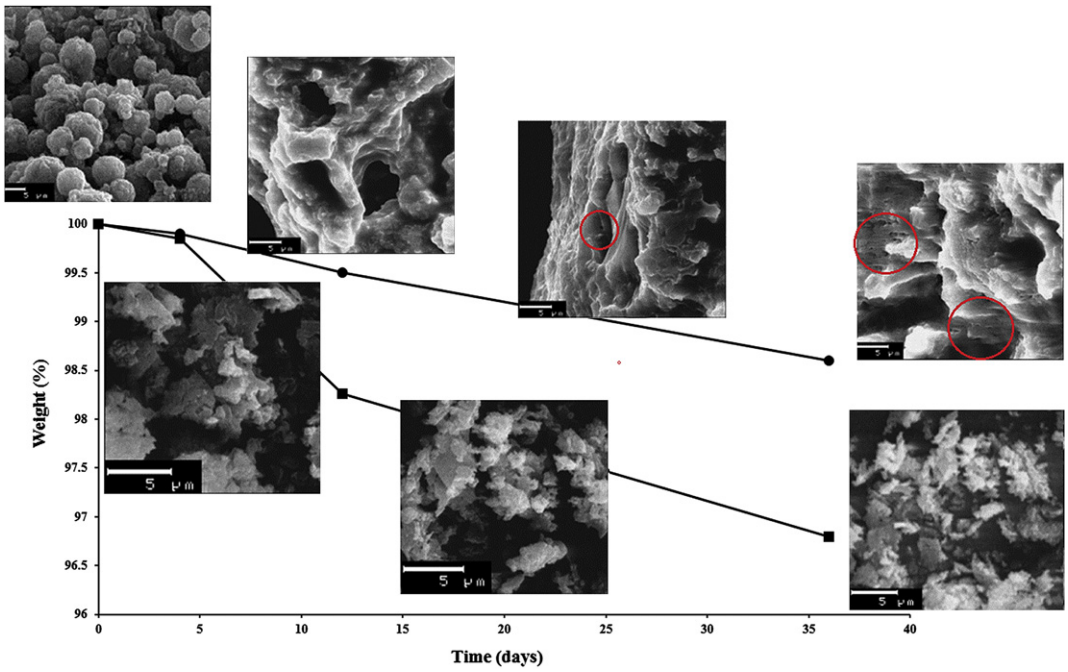

Fig. 8. The residual weight percent and surface morphology of folated nanoparticles incubated in PBS at pH 5.8 (■) and 7.4 (●) at 37 °C.

weeks incubation of these nanoparticles under pH 5.8 and 7.4, 3.2 and 1.4% decrease in mass were observed respectively.

SEM was carried out to study the surface morphology of incubated nanoparticles. The fresh nanoparticles had smooth spherical shape, while after 4 days, a dramatic change in nanoparticle shape was observed. At pH 7, nanoparticles no longer retained their spherical shape but at pH 5.8, they completely lost their spherical shape and coalesced to make a smooth film. This can be explained by the accelerated cleavage of the ester bonds under acidic conditions and their subsequent reaction with amine groups during degradation process [37]. On the 36th day, a porous surface resulted for incubated nanoparticles at pH 7.4, which implies bulk or semi-bulk degradation of nanoparticles, whereas, at pH 5.8 eroded surface was reconstructed.

4. Conclusion

Addition copolymerization of methacrylated PLGA, acrylated PEG and BOC-protected amino functional acrylate was successfully performed achieving amphiphilic and pH-sensitive brush copolymers. It was further shown that the monomers' ratio has an important role on the solubility of copolymers and their nanoparticle size. Molecular weight and hydrophilic to lipophilic balance (HLB) of copolymers could be easily controlled by adjusting the ratio of monomers in the preliminary mixture. Among different ratios, the most soluble copolymer and smallest nanoparticles were obtained from PLGA:PEG:AEMA system with 1:2:11 ratio. Folated copolymers were successfully synthesized by two-step deprotection–condensation reactions. Folated and non-folated copolymers were self-assembled into layered structures, smaller than 100 nm in diameter with a hydrophobic PLGA in the core with potent hydrophobic drug loading capability up to 13.7 wt%. The hydrophobic AEMA block contains amido-amine pendent groups and hydrolyzes when the surrounding pH is changed from neutral to acidic. Changing in pH of the medium leads to the change in nanoparticle size, morphology and characteristics of AEMA from lipophilic to hydrophilic or vice versa. Shape of the micelles in acidic pH was spherical and the sizes were below 100 nm in diameter, whereas a morphological change from spherical to bean-like shape with a large increase in size was observed in neutral media by SEM pictures. The pH-sensitive nanoparticles could deliver the pre-determined encapsulated drug more rapidly at acidic pH compared to neutral one and hence, they can be highly efficient carrier for rapid tumoricidal action. Kinetic studies confirmed that all release profiles showed two release-stages and the drug release from these nanoparticles might be controlled by Fick's laws specifically in acidic pH. It can be concluded that this kind of nanocarriers, which includes drug targeting with sensing

and therapy at the same time, has an excellent potential for the simultaneous diagnosis and therapy of cancer. Degradation studies of the copolymer were performed in buffers with varied pH values. SEM images of degraded copolymeric nanoparticles proved the degradation and suggested that surface erosion was occurred in acidic media, while, bulk erosion was observed after incubation of nanoparticles in PBS buffer at pH 7.4.

References

[1] L.E. Vlerken, M.M. Amiji, Multi-functional polymeric nanoparticles for tumour-targeted drug delivery, Expert Opin. Drug Deliv. 3 (2006) 205–216.
[2] N. Nasongkla, E. Bey, J. Ren, H. Ai, C. Khemtong, J.S. Guthi, S.F. Chin, A.D. Sherry, D.A. Boothman, J. Gao, Multifunctional polymeric micelles as cancer-targeted, MRI-ultrasensitive drug delivery systems, Nano Letters 6 (2006) 2427–2430.
[3] C. Sun, R. Sze, M. Zhang, Folic acid-PEG conjugated superparamagnetic nanoparticles for targeted cellular uptake and detection by MRI, J. Biomed. Mater. Res. 78A (2006) 550–557.
[4] M. Prabaharan, J.J. Grailer, S. Pilla, D.A. Steeber, S. Gong, Folate-conjugated amphiphilic hyperbranched block copolymers based on Boltorn (R) H40, poly(L-lactide) and poly(ethylene glycol) for tumor-targeted drug delivery, Biomaterials 30 (2009) 3009–3019.
[5] J. Hu, S. Liu, Responsive polymers for detection and sensing applications: current status and future developments, Macromolecules 43 (2010) 8315–8330.
[6] M. Wilhelm, C. Zhao, Y. Wang, R. Xu, M.A. Winnik, J. Mura, G. Riess, M.D. Croucher, Poly(styrene-ethylene oxide) block copolymer micelle formation in water: a fluorescence probe study, Macromolecules 24 (1991) 1033–1040.
[7] P.S. Low, A.C. Antony, Folate receptor-targeted drugs for cancer and inflammatory diseases, Adv. Drug Deliv. Rev. 56 (2004) 1055–1058.
[8] S. Khoee, S. Hassanzadeh, B. Goliaie, Effects of hydrophobic drug–polyesteric core interactions on drug loading and release properties of poly(ethylene glycol) polyester poly(ethylene glycol) triblock core shell nanoparticles, Nanotechnology 18 (2007) 175602.
[9] S. Khoee, M.T. Hossainzadeh, Effect of O/S/W process parameters on 17β-EV loaded nanoparticles properties, Colloids Surf. B Biointerfaces 75 (2010) 133–140.
[10] S. Khoee, H.B. Rahimi, Intermolecular interaction and morphology investigation of drug loaded ABA-triblock copolymers with different hydrophilic/lipophilic ratios, Bioorg. Med. Chem. 18 (2010) 7283–7290.
[11] T.M. Allen, Ligand-targeted therapeutics in anticancer therapy, Nat. Rev. Cancer 2 (2002) 750–763.
[12] K. Pal, S. Pore, S. Sinha, R. Janardhanan, D. Mukhopadhyay, R. Banerjee, Structure-activity study to develop cationic lipid-conjugated haloperidol derivatives as a new class of anticancer therapeutics, J. Med. Chem. 54 (2011) 2378–2390.
[13] S. Wang, E.E. Dormidontova, Nanoparticle design optimization for enhanced targeting: Monte Carlo simulations, Biomacromolecules 11 (2010) 1785–1795.
[14] N. Nasongkla, X. Shuai, H. Ai, B.D. Weinberg, J. Pink, D.A. Boothman, J. Gao, cRGD-functionalized polymer micelles for targeted doxorubicin delivery, Angew. Chem. Int. Ed. 43 (2004) 6323–6327.
[15] P.A. Bertin, J.M. Gibbs, C.K.F. Shen, C.S. Thaxton, W.A. Russin, C.A. Mirkin, S.T. Nguyen, Multifunctional polymeric nanoparticles from diverse bioactive agents, J. Am. Chem. Soc. 128 (2006) 4168–4169.
[16] V.P. Torchilin, A.N. Lukyanov, Z.G. Gao, B. Papahadjopoulos-Sternberg, Immunomicelles: targeted pharmaceutical carriers for poorly soluble drugs, Proc. Natl. Acad. Sci. U.S.A. 100 (2003) 6039–6044.
[17] V.A. Sethurame, Y.H. Bae, TAT peptide-based micelle system for potential active targeting of anti-cancer agents to acidic solid tumors, J. Control Release 118 (2007) 216–224.
[18] J.F. Ross, P.K. Chaudhuri, M. Ratnam, Differential regulation of folate receptor isoforms in normal and malignant tissues in vivo and in established cell lines. Physiologic and clinical implications, Cancer 73 (1994) 2432–2443.
[19] G. Russell-Jones, K. McTavish, J. McEwan, J. Rice, D. Nowotnik, Vitamin-mediated targeting as a potential mechanism to increase drug uptake by tumours, J. Inorg. Biochem. 98 (2004) 1625–1633.
[20] H. Li, Y. Lu, L. Piao, J. Wu, X. Yang, S.V. Kondadasula, W.E. Carson, R.J. Lee, Folate-immunoglobulin G as an anticancer therapeutic antibody, Bioconjug. Chem. 21 (2010) 961–968.
[21] D.S.W. Benoit, S. Srinivasan, A.D. Shubin, P.S. Stayton, Synthesis of folate-functionalized RAFT polymers for targeted siRNA delivery, Biomacromolecules 12 (2011) 2708–2714.
[22] S.Q. Liu, Y.W. Tong, Y.Y. Yang, Incorporation and in vitro release of doxorubicin in thermally sensitive micelles made from poly(*N*-isopropylacrylamide-*co*-*N*,*N*-dimethylacrylamide)-b-poly(D, L-lactide-*co*-glycolide) with varying compositions, Biomaterials 26 (2005) 5064–5074.
[23] E.S. Lee, H.J. Shin, K. Na, Y.H. Bae, Poly(L-histidine)-PEG block copolymer micelles and pH-induced destabilization, J. Control Release 90 (2003) 363–374.
[24] M. Soleimani, J.C. Haley, D. Majonis, G. Guerin, W. Lau, M.A. Winnik, Smart polymer nanoparticles designed for environmentally compliant coatings, J. Am. Chem. Soc. 133 (2011) 11299–11307.
[25] L. Fan, F. Li, H. Zhang, Y. Wang, C. Cheng, X. Li, C. Gu, Q. Yang, H. Wu, S. Zhang, Co-delivery of PDTC and doxorubicin by multifunctional micellar nanoparticles to achieve active targeted drug delivery and overcome multidrug resistance, Biomaterials 31 (2010) 5634–5642.
[26] J. Li, W.J. Kao, Synthesis of polyethylene glycol (PEG) derivatives and PEGylated-peptide biopolymer conjugates, Biomacromolecules 4 (2003) 1055–1067.
[27] J. Mohammadi-Rovshandeh, M.N. Sarbolouki, Synthesis and in-vitro hydrolytic degradation of polyglycolide and its L-lactide copolymer, Iran. Polym. J. 10 (2001) 53–58.
[28] C.W. Park, S.J. Lee, D. Kim, D.S. Lee, S.C. Kim, Micelle formation and sol–gel transition behavior of comb-like amphiphilic poly((PLGA-b-PEG)MA) copolymers, J. Polym. Sci. Polym. Chem. 46 (2008) 1954–1963.
[29] T. Reschel, C. Konak, D. Oupicky, L.W. Seymour, K. Ulbrich, Physical properties and in vitro transfection efficiency of gene delivery vectors based on complexes of DNA with synthetic polycations, J. Control Release 81 (2002) 201–217.
[30] D. Dube, M. Francis, J.C. Leroux, F.M. Winnik, Preparation and tumor cell uptake of poly(*N*-isopropylacrylamide) folate conjugates, Bioconjug. Chem. 13 (2002) 685–692.
[31] T. Higuchi, Mechanism of sustained-action medication. Theoretical analysis of rate of release of solid drugs dispersed in solid matrices, J. Pharm. Sci. 52 (1963) 1145–1149.
[32] R.W. Korsmeyer, R. Gurny, E. Doelker, P. Buri, N.A. Peppas, Mechanisms of solute release from porous hydrophilic polymers, Int. J. Pharm. 15 (1983) 25–35.
[33] J. Siepmann, N.A. Peppas, Modeling of drug release from delivery systems based on hydroxypropyl methylcellulose (HPMC), Adv. Drug Deliv. Rev. 48 (2001) 139–157.
[34] F. Unger, M. Wittmar, F. Morell, T. Kissel, Branched polyesters based on poly [vinyl-3-(dialkylamino) alkylcarbamate-co-vinyl acetate-co-vinyl alcohol-graft-poly(D,L-lactide-co-glycolide): effects of polymer structure on in vitro degradation behavior, Biomaterials 29 (2008) 2007–2014.
[35] A. Gopferich, Mechanisms of polymer degradation and erosion, Biomaterials 17 (1996) 103–114.
[36] X.S. Wu, N. Wang, Synthesis, characterization, biodegradation, and drug delivery application of biodegradable lactic/glycolic acid polymers. Part II. Biodegradation, J. Biomater. Sci. Polym. Ed. 12 (2001) 21–34.
[37] Y. Liu, J. Nguyen, T. Steele, O. Merkel, T. Kissel, A new synthesis method and degradation of hyper-branched polyethylenimine grafted polycaprolactone block mono-methoxyl poly (ethylene glycol) copolymers (hyPEI-g-PCL-b-mPEG) as potential DNA delivery vectors, Polymer 50 (2009) 3895–3904.